



# Biomechanical Analysis of Mandibular Implant-Assisted Removable Partial Denture with Distal Extension

Yung-Chung Chen<sup>1,2</sup> · Chi-Lun Lin<sup>3,4</sup> · Chen-Han Yu<sup>3</sup> · Hung-Chih Chang<sup>5</sup> · Yang-Ming Lin<sup>3</sup> · Jia-Wei Lin<sup>3</sup>

Received: 14 May 2022 / Accepted: 23 June 2022 / Published online: 18 July 2022  
© Taiwanese Society of Biomedical Engineering 2022

## Abstract

**Purpose** This study aimed to evaluate the mechanical performance of mandibular implant-assisted removable partial dentures (IARPDs) on abutment teeth, supporting implants, and the mucosa. A risk assessment of patient discomfort and complications was also conducted to provide a design reference for clinical use.

**Methods** Mandibular IARPDs with distal extension were analyzed using the finite element method. The mechanical performance of IARPDs was evaluated for varying numbers of missing teeth, crown-to-root ratios of abutment teeth, and locations of occlusal rests.

**Results** When an implant was placed at the distal end, the peak von Mises stress in the cortical bone surrounding the abutment tooth was 14.8% lower than that when at the mesial end. Simultaneously, the peak von Mises stress was reduced by 76.7% over the mucosa and increased by 206.7% in the cortical bone surrounding the implant. The use of distal occlusal rests increased the peak von Mises stresses in the cortical bone surrounding the abutment tooth by 8.4% compared to that when using mesial occlusal rests. When the crown-to-root ratio of the abutment tooth increased from 1 to 1.5, the peak von Mises stress in the cortical bone surrounding the abutment tooth increased by 168.7%.

**Conclusion** An IARPD with a distal implant can reduce the risk of post-op complications. When the crown-to-root ratio of the abutment tooth is adequate, the distal occlusal rest can be used for IARPDs of distal free ends.

**Keywords** Implant-assisted removable partial denture · Finite element method · Implant position · Crown-to-root ratio · Occlusal rest

## 1 Introduction

Patients with partial edentulism can be rehabilitated with various treatment options. Clasp-retained removable partial dentures (RPDs) are less expensive than other treatment options and have been widely used clinically. Although wearing RPDs can solve the dietary problems of patients with missing teeth and improve their quality of life, they may increase the risk of dental caries and periodontal diseases [1]. When one wears an RPD, the soft tissue and underlying bone of the edentulous area may suffer from discomfort. Regular follow-up and denture adjustment are usually required for long-term RPD wearers; otherwise, improper force on the alveolar ridge can eventually lead to bone resorption eventually [2]. Owing to these inconveniences, most patients with partial edentulism are not favored to wear RPDs.

IARPDs are combinations of dental implants and RPDs. This treatment option prevents the use of the alveolar ridge

✉ Chi-Lun Lin  
linc@ncku.edu.tw

<sup>1</sup> School of Dentistry & Institute of Oral Medicine, College of Medicine, National Cheng Kung University, Tainan, Taiwan, ROC

<sup>2</sup> Division of Prosthodontics, Department of Stomatology, National Cheng Kung University Hospital, College of Medicine, National Cheng Kung University, Tainan, Taiwan, ROC

<sup>3</sup> Department of Mechanical Engineering, National Cheng Kung University, Tainan, Taiwan, ROC

<sup>4</sup> Medical Device Innovation Center, National Cheng Kung University, Tainan, Taiwan, ROC

<sup>5</sup> Department of Biomedical Engineering, Hungkuang University, Taichung, Taiwan

as a support and reduces the risk of bone resorption due to improper force on the alveolar bone [3]. However, fractures of denture components and breakage or loosening of dental implants have been reported [4]. Bone resorption in the residual ridge and peri-implant mucositis were also recorded using IARPDs [5]. The survival rate of implants after ten years was 92%, and 25 of 41 patients had dental prosthesis restorations [6]. Further investigation is required to reduce late implant failure and repeated maintenance appointments. Therefore, risk assessment using IARPDs is critical.

To measure and analyze the pressure and displacement of a mandibular Kennedy classification I IARPD, Ohkubo et al. [7] installed five sensors on a physical model and inserted the implants in the bilateral second molar areas. The results showed that the implant support helped prevent the displacement of IARPDs with distal extension and decreased the pressure on the soft tissues. Matsudate et al. [8] fabricated a unilateral mandibular simulation model with a distally extended edentulous area. Piezoelectric force transducers were inserted into the root of the abutment tooth and implants, and a pressure-sensitive tactile sensor film was placed on the artificial mucosa to measure loads. A vertical load of 100 N was applied to the first molar. In the experiment, measurements were made with the conventional RPD, IARPD with a mesial implant, and IARPD with a distal implant. Consequently, the distal implant greatly reduced the load on the residual ridge. However, the load on the abutment teeth of the IARPD with a distal implant was greater than that of the conventional RPD. Ohyama et al. [9] assessed the mechanical effects of implant position and abutment height on abutment teeth, dentures, and residual ridges. The use of distal implants and increasing the height of abutment teeth can reduce the displacement of the denture base and abutment teeth.

Although previous studies have revealed the influence of implant position on the stress behavior of IARPDs, many factors still affect the load on the abutment tooth, implant, and residual ridge. These factors include the partially edentulous configuration, quality of the alveolar bone, crown-to-root ratio of the abutment tooth, viscoelasticity of the mucosa, and the type of attachments on the implant [8]. To extend the knowledge for designing IARPDs, this study aimed to evaluate the implant position of Kennedy classification II IARPDs by analyzing different numbers of missing teeth, locations of occlusal rests, and crown-root ratios of abutment teeth.

## 2 Materials and Methods

### 2.1 Geometric Modeling

In the present study, mandibular IARPDs for restoring Kennedy classification II edentulism were evaluated. All

IARPD models were designed with a single implant support to simulate clinical conditions. First, DICOM images of a human mandible were obtained from a patient (approved by the IRB of National Cheng Kung University, Taiwan, No.: A-ER-110-003) using cone-beam computed tomography (Planmeca ProMax® 3D Max, Helsinki, Finland). The images were post-processed using the computer software Mimics 16.0 (Materialise NV, Leuven, Belgium) to segment and reconstruct all parts, including teeth, periodontal ligaments, mucosa, cancellous bone, and cortical bone. To ensure reliable mesh generation in the finite element modeling, surface smoothing was applied to the reconstructed parts using the Geomagic Studio 12 software (3D Systems, Rock Hill, SC, USA).

A mandibular IARPD was digitally designed a mandibular IARPD on the reconstructed mandible. Three cases with missing teeth ( $n = 2, 3,$  and  $4$ ) were investigated. For each case, two crown-to-root ratios of the abutment tooth, 1:1 (regular) and 1.5:1 (high), were studied. The model with a high crown-to-root ratio was a modification of the regular model by trimming down the bone level surrounding the abutment tooth to simulate insufficient periodontal support. All six (two crown-to-root ratios by three cases of missing teeth) configurations were handed over to the dental technician again to design the dental prosthesis with two types (distal and mesial) of occlusal rests for each, as shown in Fig. 1. The labeled numbers shown in Fig. 1a indicate the possible implant positions in the three cases of the missing teeth. In a design configuration, a single implant was inserted into each of the possible implant positions, and the size of implant was 5 mm in diameter and 11.5 mm long in all cases.

### 2.2 Finite Element Analysis (FEA)

The pre-processing of the finite element model was performed in HyperMesh 13.0 (Altair Engineering Inc., Troy, Michigan, USA). The boundaries and contact pairs between the parts were defined to ensure that the mesh of each contact surface was closed and continuous. The 4-node tetrahedral elements (C3D4) were used, and the mesh size from 2.0 to 0.5 mm was determined by conducting a convergence analysis. The convergence analysis calculated the difference in the minimum strain by reducing the mesh size until it was less than 1%. Based on the result, 0.65 mm was used as the global mesh size, and the meshes in the region of interests were further refined. The mesh size of the peripheral ligament was set as 0.2 mm, and the mesh size of the implant, rubber and cap buckle was set as 0.1 mm. The numbers of the elements and nodes of the whole model were 3,503,833 and 741,766. The mesh model (Fig. 2) was exported as an input file and imported into the Abaqus/CAE 2017 (Dassault

**Fig. 1** Geometric models of all design configurations to be evaluated. **a** Numbers of missing teeth, **b** crown-to-root ratios, and **c** locations of occlusal rest

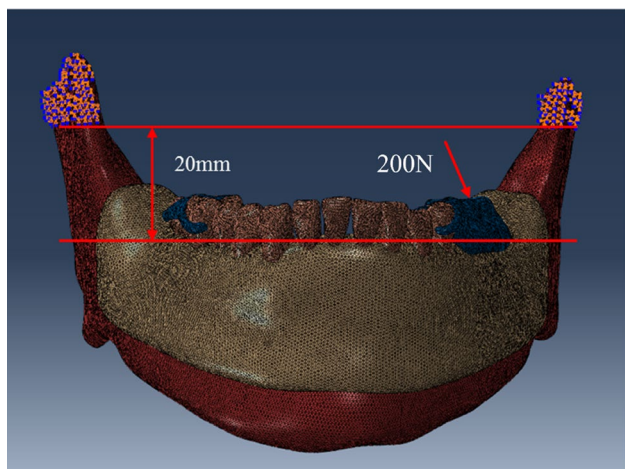
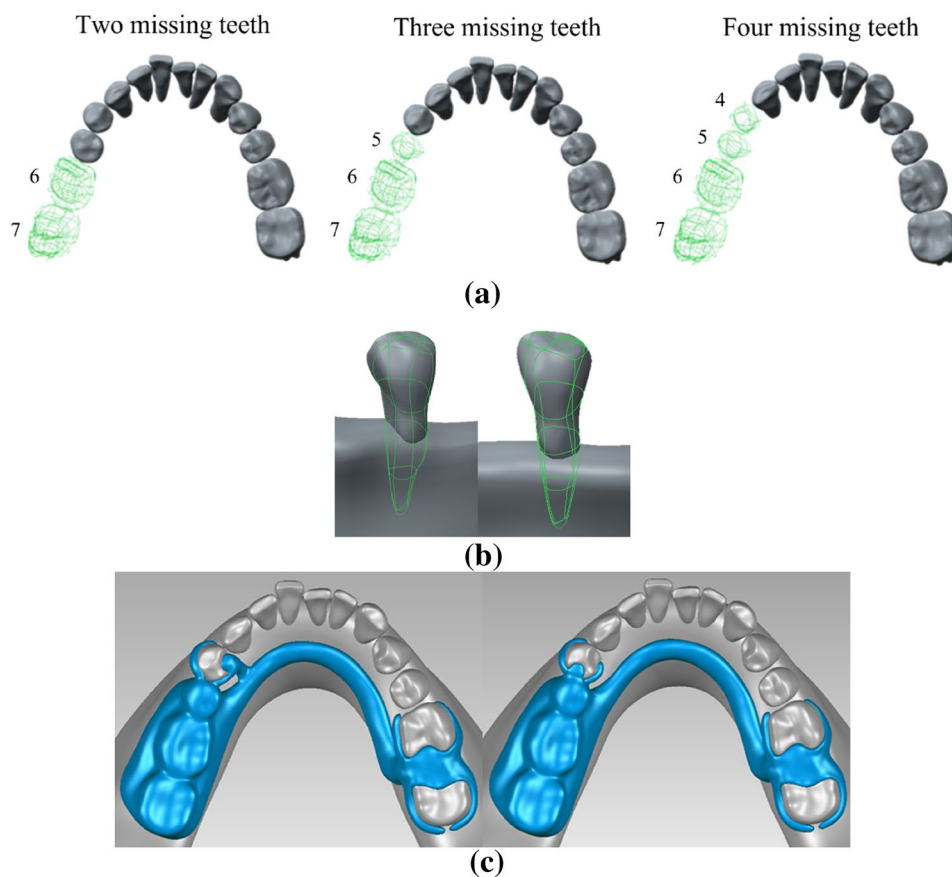


**Fig. 2** The mesh model for FEA

Systems, Johnston, RI, USA). for subsequent finite element analysis.

The finite element model incorporates mucosa, periodontal ligament, teeth, cortical bone, cancellous bone, titanium, and the denture material Pekkton® ivory. By using the PEKK material, which is ready for dental milling, we ensured that the contour of the denture remained

the same as the finite element model using the CAD/CAM technology. The material properties of each part are listed in Table 1 [10–12, 17–20]. The nodes of the cortical bone located 20 mm above the occlusal plane were fixed as the boundary conditions. An occlusal load of 200 N was applied at the second molar of the IARPD at an angle of 30-degree between the load and the long axis of the tooth, and the load was directed toward the buccal side and perpendicular to the tangent of the dentition (Fig. 2). The contact between the implant and mandible was set as a tie condition, and the other interfaces were assigned proper frictional conditions. The friction coefficients were 0.1, 0.01, and 0.36 for the interface between the occlusal rest and tooth, between the prosthesis base and mucosa, and between the implant and cap, respectively [10].

### 2.3 Biomechanical Evaluation

The peak values of the von Mises stresses of the mucosa, cortical bone at the peri-implant area, and cortical bone surrounding the abutment tooth were evaluated under different implant positions in all design configurations. The contact pressure between the mucosa and IARPD, which covered the left posterior edentulous area of the mandible, was also examined. We calculated the surface area with a pressure

higher than the threshold of 234 kPa, which could lead to mucosal pain [13]. Strains greater than 2500  $\mu\epsilon$  (tension) or smaller than  $-4000 \mu\epsilon$  (compression) [14, 15] in the cortical bone were also observed. The risk of bone loss and implant failure can be high when the bone is repeatedly subjected to strains over these thresholds.

## 2.4 In Vitro Verification Experiment

An in vitro experiment was conducted on three missing teeth with mesial occlusal rest, and the implant (Anker SBS5011) was inserted at the position of the first molar. The experimental model was fabricated using a 3D printer (Stratasys J750, Eden Prairie, MN, USA). The cortical and cancellous bones were simplified into a single part. The printing materials selected were Vero Dent Plus MED 690 for bone and Tango Plus FLX 930 for mucosa. The entire assembly of bone and mucosa materials was printed using the same manufacturing process. The abutment tooth was fabricated using zirconia and inserted into the reserved socket of the printed model. The other teeth were simultaneously printed with the same materials as the bone. To simulate the damping effect of periodontal ligaments, polyvinyl siloxane material was

injected into the socket and then a positioner was used to hold the inserted abutment tooth until the polyvinyl siloxane material set. The final model is illustrated in Fig. 3.

During the mechanical test, a ball-shaped antagonist compressed the second molar at a rate of 1 mm/min, until the force reached 200 N. Digital image correlation (DIC) was used to record the displacement of the IARPDs at five locations (No. 1–5, from mesial side to distal side) at the same vertical level, which were the centers of the three artificial teeth (the second premolar, first molar, and second molar) and two proximal contact areas between the artificial teeth. Ncorr [16], an open source 2D DIC MATLAB program, was used to perform the analyses. The DIC measurements were compared with the displacements calculated at the same five locations using FEA (Fig. 4).

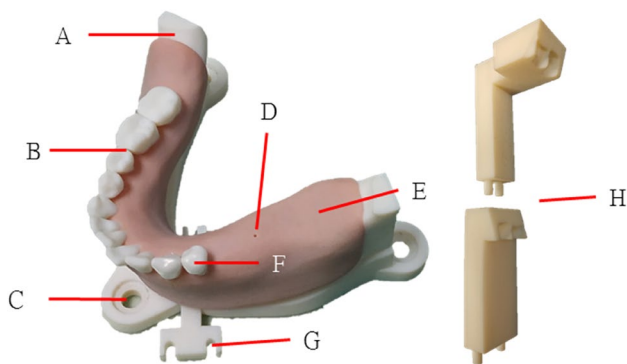
## 3 Results

### 3.1 In Vitro Verification

Comparing the five observation points in the FEA and the verification experiment, the displacements of the five measuring points along the direction of the x- and y-axes showed similar trends. However, there was a slight discrepancy between the FEA and the experiment values: approximately 0.08 mm along the x-axis and 0.25–0.3 mm along the y-axis, as shown in Fig. 5. This discrepancy resulted from the gap between the denture and mucosa in the experimental model, which caused inconsistent displacement results of the IARPD.

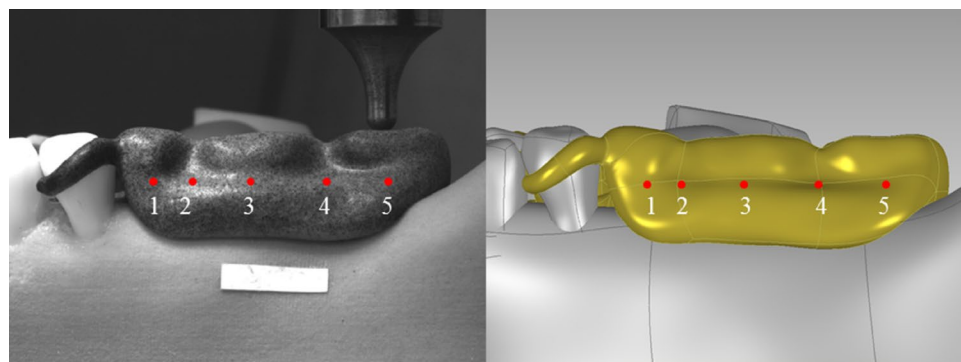
### 3.2 Stress Analysis

The stress response of the peri-implant bone area, mucosa, and surrounding abutment tooth was evaluated at different implant placement positions. The IARPD was designed with a mesial occlusal rest and a regular crown-to-root ratio. As the implant was placed more distally, the peak von Mises stress in the peri-implant bone area increased significantly.



**Fig. 3** Experimental model. A: mandibular bone, B: other teeth, C: hole for model fixation, D: implant position, E: mucosa, F: abutment tooth, G: anchor for positioner, and H: positioner for inserting abutment tooth

**Fig. 4** Observation points in DIC (left) and FEA (right)



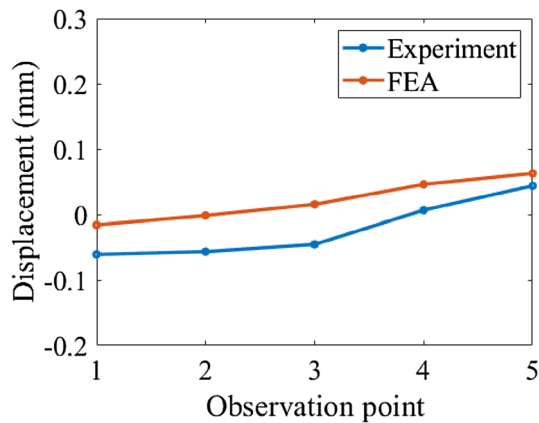


**Fig. 5** Displacements measured in FEA and verification experiment

In contrast, the stress in the bone surrounding the abutment tooth and mucosa decreased. Overall, the stresses are much larger in the peri-implant bone area than in the bone surrounding the abutment tooth and mucosa, as shown in Fig. 6.

Next, the effect of rest location was analyzed using IARPD models with a regular crown-to-root ratio. Regardless of the number of missing teeth, the difference in the peak values of von Mises stresses of the peri-implant cortical bone between the two types of occlusal rests was small (within 8.9%) (Fig. 7a). Using the IARPD with the distal occlusal rest for four missing teeth incurred larger stresses in the cortical bone surrounding the abutment tooth, whereas this difference became insignificant for those with two or three missing teeth (Fig. 7b). Regarding stress in the mucosa, the mesial occlusal rest outperformed the distal rest when the implant was placed at the first premolar area for the IARPD for four missing teeth and when the implant was placed at the second premolar area for the IARPD for three missing teeth. The distal occlusal rest performed better only when the implant was placed in the second premolar area for IARPD in four missing teeth. In the other cases, both types of occlusal rest were similar in terms of mucosal stress (Fig. 7c).

As the mesial occlusal rest is more commonly used, it was employed in this study as the base design to study the effect of crown-to-root ratio. When the crown-to-root ratio increased, the peak value of the von Mises stress of the cortical bone in the peri-implant area increased (avg. 28.4% increase, see Fig. 8a). The effect was more significant for the bone stress surrounding the abutment tooth for the IARPD for the four missing teeth (avg. 161.9% increase), but was insignificant for the IARPD for two or three missing teeth (Fig. 8b). The two crown-to-root ratios did not have a clear impact on stress in the mucosa (differences were within 0.6 MPa), regardless of the number of missing teeth (Fig. 8c).

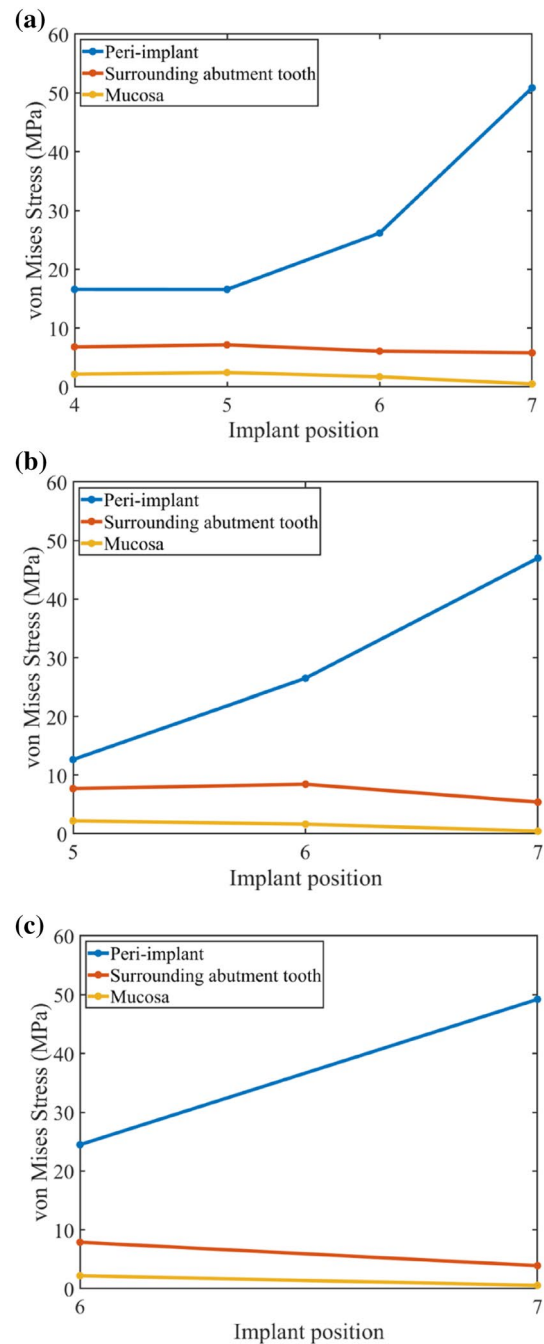


**Fig. 6** Peak von Mises stress corresponding to different implant positions observed in three regions for four (a), three (b), and two (c) missing teeth

### 3.3 Mucosa Contact Pressure

The effect of the location of occlusal rests and implant position was evaluated using models of regular crown-to-root ratio. As shown in Fig. 9, when an implant was placed at the second molar, the contact pressure over the mucosa was significantly lower in all configurations. The effect of the

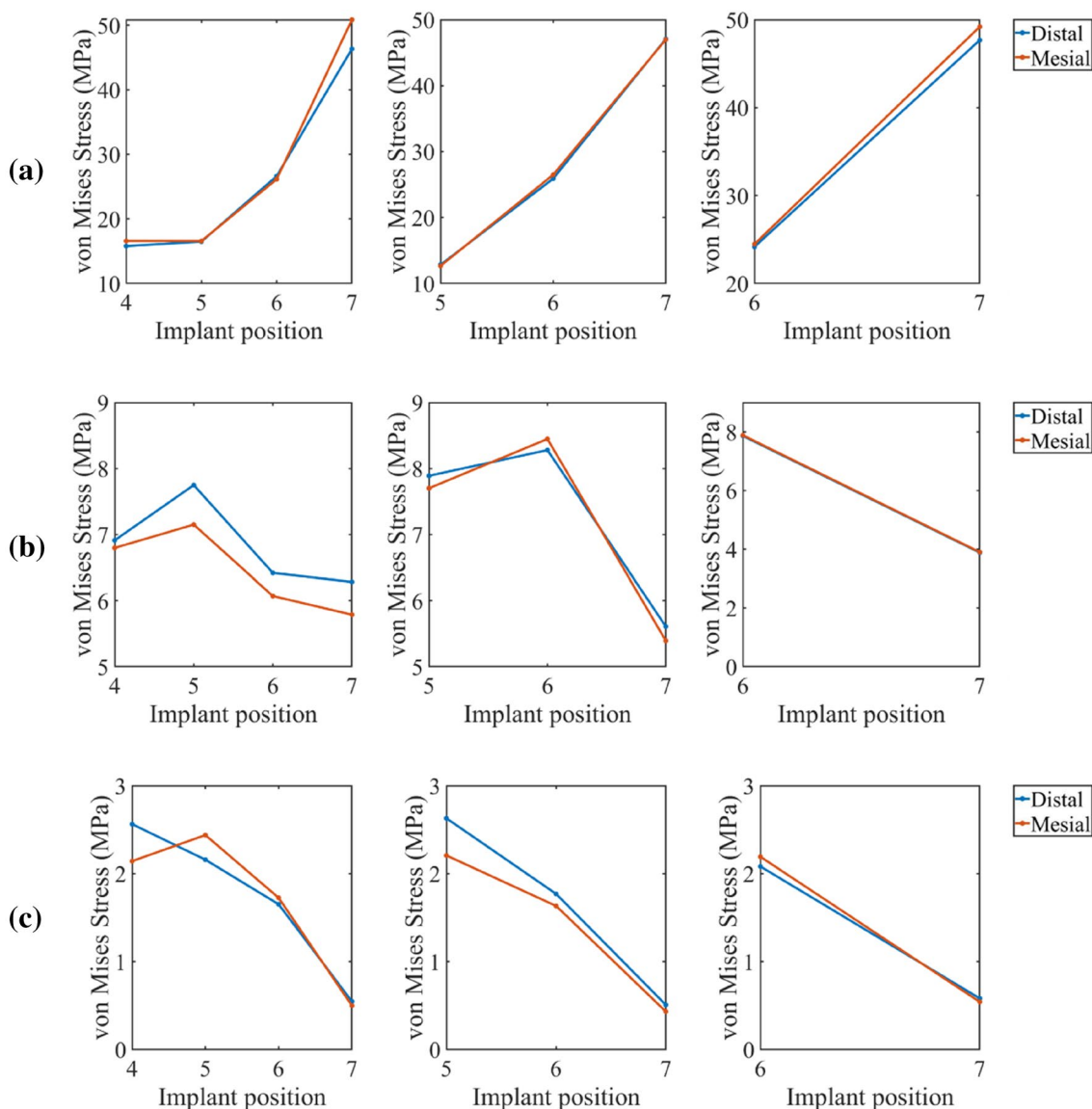


**Fig. 7** Peak von Mises stress corresponding to the two types of rest with different implant positions observed in peri-implant (a), surrounding the abutment tooth (b), and mucosa (c) regions

remaining location can be observed in two cases. One was placed in the IARPDs for four missing teeth when an implant was placed at the position of the first premolar, and the other was placed in the IARPDs for three missing teeth when an implant was placed at the position of the first molar.

**3.4 Cortical Bone Strain**

The maximum and minimum principal strains of peri-implant cortical bone were investigated for IARPD with a regular crown-to-root ratio and mesial occlusal rest. Larger strains were observed when the implant was placed

more distally. When the implant was placed in the second molar, both the maximum and minimum principal strains exceeded the threshold, as shown in Fig. 10.

**3.5 Risk of Pain Assessment**

After calculating the total area (%) of the mucosa-denture interface with a contact pressure larger than the threshold (234 kPa), the most distal implants showed better results (16.8%) than the most mesial implants (41.4%), as shown in Fig. 11.

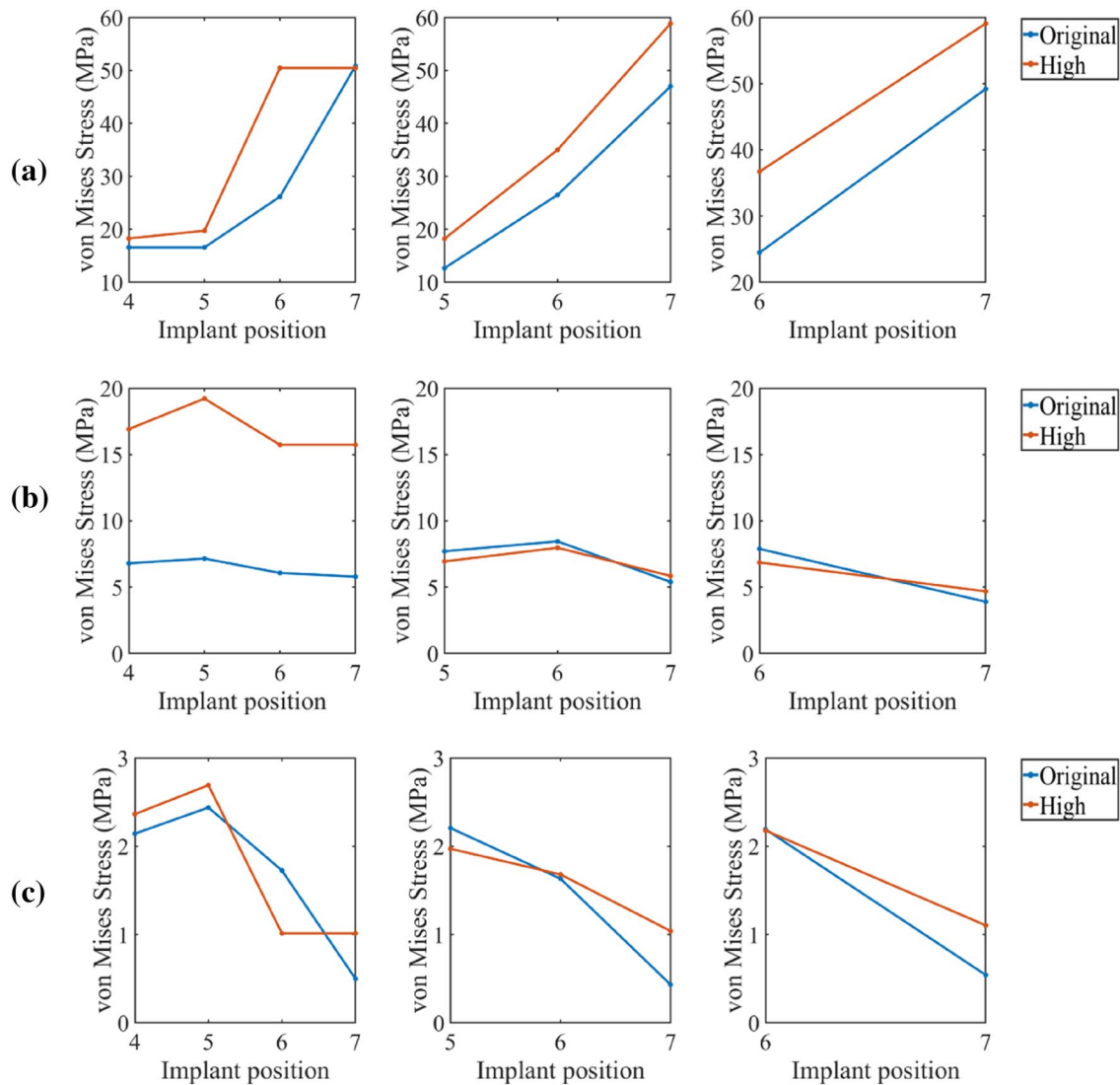


**Fig. 8** Peak von Mises stress corresponding to the two crown-to-root ratios with different implant positions observed in peri-implant (a), surrounding abutment (b), and mucosa (c) areas

## 4 Discussion

The present study evaluated the effect of implant position for IARPDs of Kennedy Classification II edentulism. Although discrepancy was found in measured displacements between FEA and verification experiment, their trends match each other. By my observation, this discrepancy was attributed to a gap between the printed denture and mucosa, which may be resulted from polishing and finishing process. Despite the gap effect, the numerical results were still in vitro validated.

The level of stress was evaluated in three regions: the peri-implant area, surrounding the abutment tooth, and mucosa, which are relevant to clinical complications. Regardless of the number of missing teeth, the effect of the implant position on stress was similar. The stress level

increased as the implant position moved from the mesial end to the distal end. Placing an implant more mesially, that is closer to the abutment tooth, enables the load on the abutment tooth to be transmitted to the implant. Consequently, the stress in the cortical bone surrounding the abutment tooth decreased.

Although placing an implant more distally increases the cortical bone stress in the peri-implant region, it could reduce the level of stress in the cortical bone surrounding the abutment tooth and mucosa. This finding is consistent with those in the literature [8]. In the present study, a load was applied to the second molar to simulate heavier chewing. Under this loading condition, when the implant was placed more distally and closer to the point of load, the bone stress surrounding the implant increased. It should be noted that

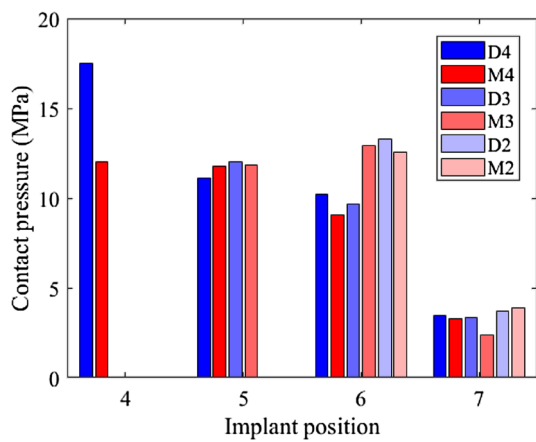


**Fig. 9** Contact pressure between the mucosa and occlusal rest. The identifiers in the legend are D: distal occlusal rest, M: mesial occlusal rest, and the digit: number of missing teeth

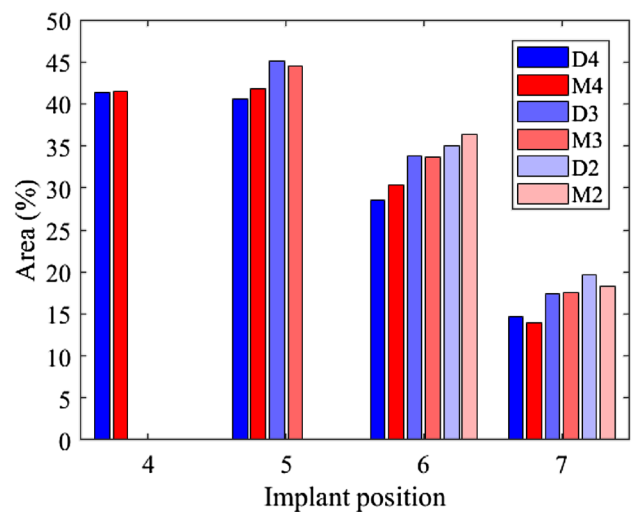


**Fig. 11** Percentage of mucosal surface area where stress threshold of pain is exceeded

increased stress may cause secondary damage to the bone, especially when the quality of the alveolar bone in the posterior region is poor.

The locations of occlusal rest had no significant effect on the stress of the cortical bone and mucosa for the two- and three-unit IARPDs. Relatively higher stresses were observed when using the distal occlusal rest for IARPD for the four missing teeth. This was because the mesial occlusal rest can better transfer the load to the abutment tooth. In addition, the mesial occlusal rest of the IARPDs used in the present study extended from the mesial side to the distal side using a crossbar. The abutment tooth was enveloped more completely, which could have increased the force on the abutment tooth. Therefore, mesial occlusal rest should be carefully used, especially when the patient's abutment tooth is periodontally unhealthy.

Increasing the crown-to-root ratio induced higher stresses in all regions for most of the cases investigated in this study. A tooth with a higher crown-to-root ratio

would have peripheral supporting bones at a lower level, which increases the moment arm. Therefore, higher bending stresses could occur at the abutment tooth and its surrounding bone area and could be further aggregated when the number of remaining teeth was low. When the number of missing teeth is reduced, the abutment tooth changes from the canine tooth to the premolars, which reduces the effect of the crown-to-root ratio on the stress response.

The mesial implant group had a larger area in which the contact pressure was greater than the pressure pain threshold, which can be attributed to the loading location. The occlusal force was applied at the second molar, and the fulcrum is at the top of the implant, and it resulted in larger contact pressure on the contact area between the load point and the implant position. Among them, the mesial implant was farther from the load point, which led to a larger area of high contact pressure below the load point. Therefore,

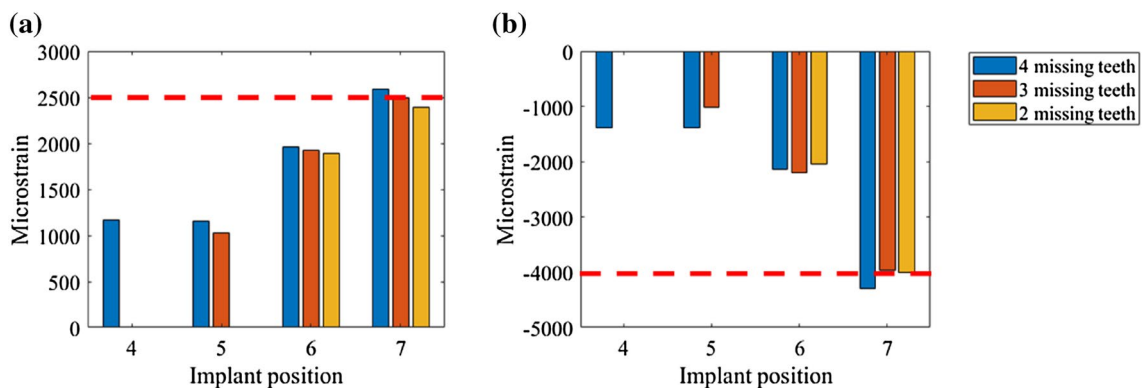


**Fig. 10** Maximum (a) and minimum (b) principal strains of peri-implant cortical bone



**Table 1** Material properties used in FEA

Part	Young's modulus (MPa)	Poisson's ratio
Mucosa (Tango Plus FLX930)	0.548 [11]	0.49
Periodontal ligament	10 [19]	0.49
Cap (Ti)	110,000 [10]	0.3
Rubber	5 [20]	0.49
Teeth	210,000 [12]	0.3
Cortical bone, Cancellous bone (Vero Dent Plus MED 690)	2372.3 [18]	0.3
Implant (Ti)	110,000 [10]	0.3
Denture material (Pekkton® ivory)	5100 [17]	0.3

when using mesial implants, the condition of the patient's mucosa should be considered to avoid discomfort.

A distal implant can effectively reduce mucosal discomfort. However, the results of the principal strain on the peri-implant cortical bone showed that the strain on the peri-implant cortical bone exceeded the bone resorption threshold when the implant was inserted at the first and second molars. Therefore, when the quality of the patient's alveolar bone is insufficient, the use of distal implants should be avoided to reduce the risk of bone resorption and ensure long-term success and prognosis.

The present study was limited to investigate the effect of implant insertion for Kennedy Classification II RPDs only. However, the effect of modification area was not considered. Moreover, RPDs for Kennedy Classification I edentulism which has distal free ends at both sides were not considered. Also implants of the same size were assumed for each case, the sizing effect of implants was not evaluated. To better design IARPDs clinically, further investigation is still required.

## 5 Conclusion

In the present study, the finite element method and a verification experiment were used to analyze the biomechanical behavior of IARPDs. The mechanical performance of the IARPDs on the abutment tooth, implant, and mucosa was investigated, as well as the risk assessment of patient discomfort and complications. Several important findings of this study can be used as references for clinical treatment design. Within the limitations of this study, the following conclusions were drawn:

- (a) Placing implants more distally can reduce the stress on the abutment tooth and mucosal discomfort but increases the risk of peri-implant bone resorption.
- (b) When the quality of alveolar bone in the posterior area is poor, the implant should not be inserted. In this case,

mesial placement of an implant might be a better option to reduce bone resorption.

- (c) An IARPD with a distal occlusal rest and a distal implant can be used, while the crown-to-root ratio is adequate.
- (d) In Kennedy classification II partial edentulism, the number of missing teeth has little effect on the stress behavior of the IARPD.

**Acknowledgements** The authors would like to thank Professor Dr. Chih-Han Chang and for his guidance and the experimental instruments support in this research.

**Funding** This work was supported by the Ministry of Science and Technology, Taiwan (Grant number 07-2221-E-006-052-MY2).

## Declarations

**Competing interests** The authors have no relevant financial or non-financial interests to disclose.

## References

1. Vermeulen, A., et al. (1996). Ten-year evaluation of removable partial dentures: Survival rates based on retreatment, not wearing and replacement. *The Journal of Prosthetic Dentistry*, 76(3), 267–272.
2. Teitelbaum, S. L. (2000). Bone resorption by osteoclasts. *Science*, 289(5484), 1504–1508.
3. Keltjens, H. M., et al. (1993). Distal extension removable partial dentures supported by implants and residual teeth: Considerations and case reports. *International Journal of Oral & Maxillofacial Implants*, 8(2), 208–213.
4. De Freitas, R., et al. (2012). Mandibular implant-supported removable partial denture with distal extension: A systematic review. *Journal of Oral Rehabilitation*, 39(10), 791–798.
5. Threeburuth, W., Aunmeungtong, W., & Khongkhunthian, P. (2018). Comparison of immediate-load mini dental implants and conventional-size dental implants to retain mandibular Kennedy class I removable partial dentures: A randomized clinical trial. *Clinical Implant Dentistry and Related Research*, 20(5), 785–792.

6. Payne, A. G., et al. (2017). Multicentre prospective evaluation of implant-assisted mandibular removable partial dentures: Surgical and prosthodontic outcomes. *Clinical Oral Implants Research*, 28(1), 116–125.
7. Ohkubo, C., et al. (2007). Effect of implant support on distal extension removable partial dentures: In vitro assessment. *Journal of Oral Rehabilitation*, 34(1), 52–56.
8. Matsudate, Y., et al. (2016). Load distribution on abutment tooth, implant and residual ridge with distal-extension implant-supported removable partial denture. *Journal of Prosthodontic Research*, 60(4), 282–288.
9. Ohyama, T., et al. (2020). Mechanical analysis of the effects of implant position and abutment height on implant-assisted removable partial dentures. *Journal of Prosthodontic Research*, 64(3), 340–345.
10. Shahmiri, R., & Das, R. (2017). Finite element analysis of implant-assisted removable partial dentures: Framework design considerations. *The Journal of Prosthetic Dentistry*, 118(2), 177–186.
11. Abtan, A. A., et al. (2016). Analyzing the 3D printed material Tango plus FLX930 for using in self-folding structure. 2016 *International Conference for Students on Applied Engineering (ICSAE)*.
12. Chen, F., et al. (2020). Preparation and biological evaluation of ZrO<sub>2</sub> all-ceramic teeth by DLP technology. *Ceramics International*, 46(8), 11268–11274.
13. Ogawa, T., et al. (2004). Mapping, profiling and clustering of pressure pain threshold (PPT) in edentulous oral mucosa. *Journal of Dentistry*, 32(3), 219–228.
14. Misch, C. E. (2014). *Dental implant prosthetics-e-book*. Amsterdam: Elsevier Health Sciences.
15. Pattin, C., Caler, W., & Carter, D. (1996). Cyclic mechanical property degradation during fatigue loading of cortical bone. *Journal of Biomechanics*, 29(1), 69–79.
16. Blaber, J., et al. (2015). Ncorr: open-source 2D digital image correlation Matlab software. *Experimental Mechanics*, 55(6), 1105–1122.
17. Cendres+Métaux. Pekkton® ivory. <https://www.cmsa.ch/en/medtech/products/estheticline/high-performance-polymers/pekkton-ivory/>
18. Stratasys. Vero Dent Plus MED690. [https://www.stratasys.com/materials/search/dentalmaterials?utm\\_source=data-sheet&utm\\_medium=pdf&utm\\_content=dental-materials-data-sheet-link-4-verodentplus-med690](https://www.stratasys.com/materials/search/dentalmaterials?utm_source=data-sheet&utm_medium=pdf&utm_content=dental-materials-data-sheet-link-4-verodentplus-med690)
19. Rees, J. S., & Jacobsen, P. H. (1997). Elastic modulus of the periodontal ligament. *Biomaterials*, 18(14), 995–999.
20. Barão, V. A., et al. (2013). Comparison of different designs of implant-retained overdentures and fixed full-arch implant-supported prosthesis on stress distribution in edentulous mandible—a computed tomography-based three-dimensional finite element analysis. *Journal of Biomechanics*, 46(7), 1312–1320.